Magnetoluminescence from strain-induced quantum dots

M. Braskén and M. Lindberg
Department of Physics, Åbo Akademi University, 20500 Turku, Finland

J. Tulkki
Optoelectronics Laboratory, Helsinki University of Technology, 02150 Espoo, Finland

(Received 15 October 1996; revised manuscript received 23 December 1996)

We have calculated the effects of valence-band coupling on the magnetoluminescence spectra from an $In_xGa_{1-x}As/GaAs$ quantum-well dot induced by an InP stressor island. The theory is based on the single-particle Luttinger-Kohn Hamiltonian using a realistic confinement potential. The band coupling strongly influences the calculated spectra. The numerical results were compared with experiments and a good agreement was obtained. Numerical results predict a reversal of the mesoscopic Zeeman splitting for the ground state and an avoided crossing of excited states. [S0163-1829(97)12016-1]

Recently an approach to fabricate quantum dots (QD) of high optical quality has been introduced by Lipsanen *et al.*[1] The three-dimensional (3D) confinement is obtained by self-organized growth of InP islands with very homogeneous size distribution on the surface of an $In_xGa_{1-x}As/GaAs$ quantum well (QW). A local 3D energy minimum appears inside the $In_xGa_{1-x}As$ layer under an InP island, forming an effective QD free of any damage caused by the processing. The reduced inhomogeneous broadening in these QD's has made it possible to resolve several excited energy levels as separate spectral lines in the luminescence spectrum. A well resolved magnetoluminescence spectrum displaying a diamagnetic shift of the ground-state line and a prominent splitting of the first excited state line was measured in these structures by Rinaldi *et al.*[2] In similar measurements in etched $In_xGa_{1-x}As/GaAs$ QD structures reported by Bayer *et al.*,[3] the energy levels were not resolved.

The magnetic interactions have been previously studied mainly in field effect quantum dots, which confine only electrons. Recently Darnhofer *et al.*[4] have considered theoretically the far infrared absorption (FIR) of QD's confining holes only. Their analysis, assuming a parabolic lateral confinement, accounted for band coupling and predicted the existence of an anticrossing of spectral lines in the absorption spectrum. However, since the FIR spectrum involves dipole allowed *intraband* transitions, the results presented in Refs. 4 and 5 cannot be used as such to analyze magnetoluminescence spectra involving *interband* transitions.

In this work we will extend the calculations presented in Refs. 2 and 6 by analyzing, within the coupled valence-band model, the magnetic interactions in QD's confining both electrons and holes. The confinement potential is assumed axially symmetric but not necessarily parabolic, nor mirror symmetric vertically. Also the general conservation laws and symmetry effects governing the interband radiative recombination in strain induced QD's are investigated. The results are compared with the experimental data of Rinaldi *et al.*[2]

In the materials we are considering, the valence bands are characterized by an atomic angular momentum $J=3/2$, formed by coupling the spin and the angular momentum of the p-type band orbital. The Luttinger-Kohn Hamiltonian including the strain-induced confinement and the magnetic field[7] is then given by

$$H=\begin{pmatrix} H_{\mathrm{HH}}+V_{\mathrm{HH}} & b & c & 0 \\ b^{\dagger} & H_{\mathrm{LH}}+V_{\mathrm{LH}} & 0 & c \\ c^{\dagger} & 0 & H_{\mathrm{LH}}+V_{\mathrm{LH}} & -b \\ 0 & c^{\dagger} & -b^{\dagger} & H_{\mathrm{HH}}+V_{\mathrm{HH}} \end{pmatrix} + \frac{e}{m_0}\kappa B J_z, \tag{1a}$$

$$H_{\mathrm{HH,\,LH}}=\frac{-\hbar^2}{2m_0}\left[(\gamma_1\mp 2\gamma_2)\frac{\partial^2}{\partial z^2}+(\gamma_1\pm\gamma_2)\left(\frac{\partial^2}{\partial x^2}+\frac{\partial^2}{\partial y^2} -2\frac{\overline{\omega}}{\hbar}\hat{L}_z-\overline{\omega^2}(x^2+y^2)\right)\right], \tag{1b}$$

$$b=-\frac{\sqrt{3}\hbar^2}{m_0}\gamma_3\frac{\partial}{\partial z}\left(\frac{\partial}{\partial x}-i\frac{\partial}{\partial y}+\overline{\omega}(x-iy)\right), \tag{1c}$$

$$c=\frac{\sqrt{3}\hbar^2}{2m_0}\frac{\gamma_2+\gamma_3}{2}\left(\frac{\partial}{\partial x}-i\frac{\partial}{\partial y}+\overline{\omega}(x-iy)\right)^2, \tag{1d}$$

where m_0 is the bare electron mass and $\overline{\omega}=eB/2\hbar$. In Eq. (1b) and below the upper (lower) sign corresponds to heavy hole (light hole) [HH (LH)]. The nondiagonal terms of the Pikus-Bir strain Hamiltonian[8] were found to be small, especially for the few lowest states, and the HH and LH confinement potentials are given by $V_{\mathrm{HH,LH}}(r,z)=V_h^{\mathrm{QW}}(z)+V_h^H(r,z)\pm V_h^S(r,z)$, where $V_h^{\mathrm{QW}}(z)$ is the hole band edge confinement potential, $V_h^H(r,z)=a_\nu(e_{xx}+e_{yy}+e_{zz})$ the hydrostatic deformation potential, and $V_h^S(r,z)=b_\nu[e_{zz}-(e_{xx}+e_{yy})/2]$ the shear deformation potential. The thickness of the $In_{0.1}Ga_{0.9}As/GaAs$ QW (7 nm) and the cladding layer (5 nm) as well as the dimensions of the cylindrically symmetric InP island, bottom radius 40 nm, top radius 30 nm, and height 20 nm, correspond to the sample used in the experiment of Rinaldi *et al.*[2]

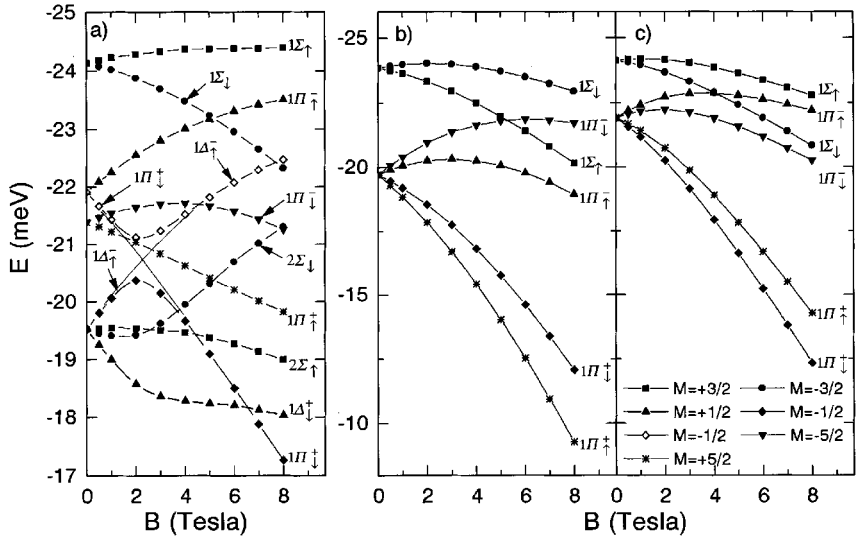

FIG. 1. The valence-band dispersion as a function of the field strength. (a) Numerical calculation including the band coupling, (b) numerical calculation excluding the band coupling, and (c) analytical values normalized to the numerical calculations at $B=0$. Anticrossing states in the case of a vertically mirror symmetric QW potential denoted by dashed lines. The zero of the hole energy is at the QW HH1 state.

The z component of the total angular momentum, $\hat{J}_{\mathrm{tot}}=\hat{J}_z+\hat{L}_z$, where $\hat{L}_z$ is the mesoscopic angular momentum, is a conserved quantity. The four-component envelope function in cylindrical coordinates is of the form $\psi_{m_j}(r,z,\phi)=e^{i(M-m_j)\phi}\chi_{m_j}(r,z)$, where $\hbar M$ is the eigenvalue of the z component of the total angular momentum. M must be a positive or negative half-integer (but not an integer) and m_j takes the values $\pm 3/2, \pm 1/2$.

When the width of the top barrier layer of the QW structure is increased, both the QW band edge potential and the strain-induced potential become approximately mirror symmetric relative to the center plane of the QW. In this limit the eigenstates can be assigned a definite parity. The eigenvalues of the inversion operator P are ± 1, and in the corresponding energy eigenstate the $\pm 3/2$ and $\mp 1/2$ components are even in z and the $\mp 3/2$ and $\pm 1/2$ components are odd.

The numerical calculation of the eigenvalues and eigenfunctions of Eq. (1a) consists of the following four steps: (i) Determining the strain from the theory of elasticity, (ii) converting the strain into a deformation potential according to the theory of Pikus and Bir,[8] (iii) adding the deformation potential to the band edge confinement potential to produce the total potentials appearing in the envelope Hamiltonian, and (iv) solving the resulting eigenvalue problem numerically using the finite element method.

By studying the magnitudes of the four components $m_j=\pm 3/2, \pm 1/2$ of the valence-band envelope functions, we found that either the $m_j=3/2$ or $m_j=-3/2$ component is much larger (in absolute value) than the other components. However, we use the expressions ''HH- and LH-*like* states'' because the band coupling plays an important role. The compressive strain in the $\mathrm{In}_x\mathrm{Ga}_{1-x}\mathrm{As}$ well layer lifts the energies of the LH-like states clearly above the first few excited HH-like states. The total effective potential for the LH's is above the GaAs band edge and, therefore, it is questionable if the LH-like states are confined in the QD, or even in the QW. Because the coupling between the HH and LH states is reduced, the mesoscopic angular momentum is approximately a constant of motion. Therefore, a mesoscopic angular momentum number m is a useful tool to identify eigenstates from the experimental spectrum and we can label the valence-band states by $N\Sigma_{\uparrow\downarrow}, N\Pi^{\pm}_{\uparrow\downarrow}, N\Delta^{\pm}_{\uparrow\downarrow}, \ldots$ in analogy to the electron states.

The mesoscopic angular momentum number m is defined as the nearest integer to $\langle \hat{L}_z\rangle/\hbar$ and used as a label for the valence-band state. We can have $M\approx m+3/2$ or $M'\approx m-3/2$ corresponding to the same m: both states exist and have different wave functions and energies. Whenever the $\chi_{\pm 3/2}$ component dominates, we have $\langle \hat{S}_z\rangle\approx \pm 1/2\hbar$, respectively. We denote the dominant HH component by $\uparrow(\downarrow)$ for $m_j=3/2(-3/2)$. The numerical calculations showed that this leads to $m=M-3/2$ for the $\uparrow$ states and $m=M+3/2$ for the $\downarrow$ states.

For the valence band the calculated magnetic field behavior becomes rather complex when the band coupling is included, as shown in Fig. 1(a). As for the conduction band (with spin included), the HH-like states at $B=0$ form groups with approximate degeneracies, 2, 4, 6, ..., starting from the ground state. In Fig. 1(b) all off-diagonal terms in Eq. (1a) have been set to zero and the result is similar to the conduction-band case (not shown). The coupling drastically changes the magnetic field dependence of the energy levels, especially for the excited states.

The magnetic field dependence of the HH-like states is dominated by the linear Zeeman-like behavior, which is related to the mesoscopic angular momentum (the contribution from the atomic Zeeman term is small). The numerical results show that also the two lowest states have a weak linear B dependence. The B dependence and the removal of degeneracy are due to the band coupling.

Since the confinement in the z direction is strong, for an analytic approximation it is reasonable to assume, for the first few QD states, that the well potential is infinite and that only the ground state of the QW is important. The radial confinement potential is not as strong, but can be approximated by a parabolic potential close to the minimum of the potential. In this limit the momentum p_z is large and of the order of $\sqrt{\gamma_1}\hbar/L\approx\sqrt{2m_0E_z^0}$, where L is the well width. In the second-order perturbation theory the problem splits into two independent blocks for the states with angular momenta

$(3/2,1/2)$ and $(-3/2,-1/2)$, respectively. The expansion gives the approximate spectrum for the HH states in the form

$$E_{n,m}^{\pm 3/2}=E_z^0\pm\Delta\hbar\omega_B^0\pm\frac{3}{2}\kappa\omega_B^0+(\gamma_1+\gamma_2+2\Delta)$$

$$\times\left(\hbar\omega_c(2n+|m|+1)+\hbar\frac{\omega_B^0}{2}m\right), \tag{2}$$

where $\omega_B^0=eB/m_0$ is the bare cyclotron frequency and $\omega_c=\sqrt{\xi/m_0(\gamma_1+\gamma_2+2\Delta)+(\omega_B^0/2)^2}$, ξ being the strength of the parabolic confinement. For an infinite rectangular potential well in the z direction,

$$\Delta=-\frac{3\gamma_3^2}{2\pi\gamma_2}\left(\frac{4\pi}{1-b^2}-\frac{16b\cot(\pi b/2)}{(1-b^2)^2}\right), \tag{3}$$

where $b=(\gamma_1+2\gamma_2)^{-1/2}\sqrt{\gamma_1-2\gamma_2-(E_{\mathrm{LH}}^0-E_{\mathrm{HH}}^0)/E_z^0}$. The exact value of Δ depends on the actual form of the potential. These expressions, even if not numerically accurate, show [see Fig. 1(c)] that the ground-state degeneracy $(n=m=0)$ is broken and a splitting linear in B appears because of the second term on the right-hand side of Eq. (2). If the band coupling is neglected by setting off-diagonal elements to zero, the ground state becomes degenerate (except for the small splitting due to the atomic Zeeman term) in analogy to the conduction band. If the atomic Zeeman term dominated, the splitting of the ground states would be in the reversed order. This reversing was not observed in experiments by Bayer *et al.*[9] for etched $In_{0.1}Ga_{0.9}As/GaAs$ QD structures. However, in these materials the effective carrier potentials are very different from those in the strain-induced QD's studied here. For excited states with nonzero mesoscopic angular momentum, the last terms in Eq. (2) dominate in the linear splitting of the states, because $\Delta/\gamma_1\approx 1/10$ in our approximation.

Around $B=2$ T, where one of the $m=+1$ levels meets an $m=-2$ level from the next group, we see an avoided crossing. Both levels correspond to $M=-1/2(M+3/2=+1, M-3/2=-2)$, which makes the avoided crossing possible. In a mirror symmetric potential the levels would cross because they would have different parities. In our case, however, the potential is slightly asymmetric in the z direction and the crossing is avoided because the parity is not conserved exactly and mixing of states with different parities is possible.

By following the lower of the $M=-1/2$ levels [solid diamonds in Fig. 1(a)], which at $B=0$ corresponds to $m=+1$, we can observe how the dominant component changes from $\chi_{3/2}$ to $\chi_{-3/2}$, when the level goes through the avoided crossing and changes to $m=-2$. An experimental observation of the avoided crossing in luminescence spectra would be a direct proof of the existence of the band coupling in QD's. The analog of this phenomenon in the far-infrared response of parabolic QD's has been predicted by Darnhofer *et al.*[4] Excluding these anticrossing levels, the component structure of valence-band states, governed by weight factors $\langle\chi_{m_j}|\chi_{m_j}\rangle$, changes only slightly as a function of field strength. Typically the weight of the $\chi_{3/2}$ component in the $1\Sigma_\uparrow$ state decreased gradually from 0.98 at $B=0$ to 0.92 at $B=6$ T.

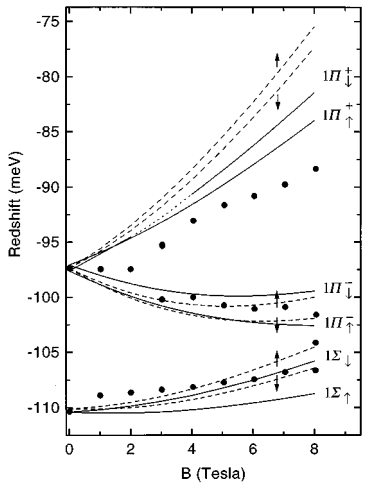

FIG. 2. The luminescence energies for the ground states and the lowest excited states. Calculation with coupled bands (solid line), single band calculation (dashed line), and experimental data (solid dots).j The arrows at $B=77$ correspond to the spin states of the single band calculation.

The luminescence intensity is given by

$$I\propto\left|\boldsymbol{\epsilon}\cdot\sum_{sm_j}\boldsymbol{\mu}_{s,m_j}^{cv}\int\psi_s^e(\mathbf{r})\psi_{m_j}^h(\mathbf{r})\mathrm{d}\mathbf{r}\right|^2, \tag{4}$$

where $\boldsymbol{\epsilon}$ is the polarization vector of the emitted photons and s is the spin index. The envelope functions $\psi_s^e(\mathbf{r})$ and $\psi_{m_j}^h(\mathbf{r})$ correspond to conduction- and valence-band states with specified quantum numbers. The dipole matrix element $\boldsymbol{\mu}_{s,m_j}^{cv}$ is calculated using the atomic Bloch states at the Γ point. To analyze the magnetoluminescence spectra of Ref. 2 we consider a special case in which the luminescence is emitted orthogonally to the QW plane $(\epsilon_z=0)$ and the po-

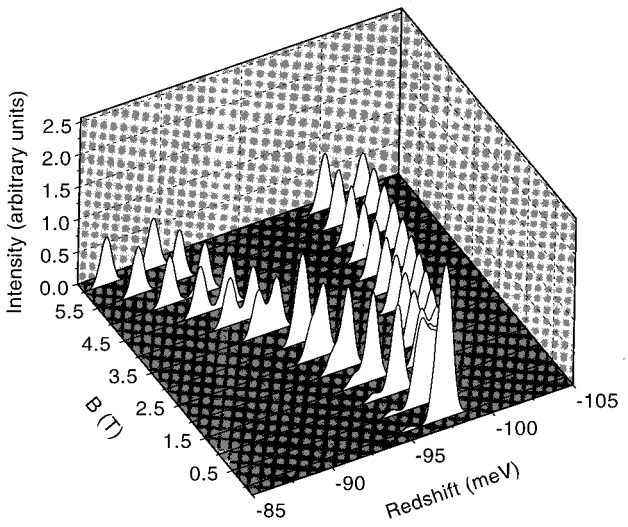

FIG. 3. The luminescence spectrum corresponding to the excited states $1\Pi_{\downarrow\uparrow}^{\pm}$ and $1\Delta_\uparrow^-$. A Lorentzian line shape with a half-width of 1 meV was assumed. The transition energy (<0) is defined as the difference between the QD and QW luminescence energies.

larizations are summed over. In the magnetic field each combination of initial and final quantum numbers corresponds to different transition energy.

In Fig. 2 we show the transition energies $E_{ei}+E_{\nu j}$ of the QD luminescence lines for the ground state and the few lowest excited states. The transitions $1\Pi^{\pm}_{\uparrow\downarrow}\rightarrow 1\Pi^{\pm}_{\uparrow\downarrow}$ and $1\Pi^{+}_{\downarrow}\rightarrow 1\Delta^{-}_{\uparrow}$ were selected because the corresponding luminescence lines are well resolved in the experiment of Rinaldi *et al.*[2] Figure 2 shows that the inclusion of the band coupling (solid line) leads to a much better agreement with experiment. The single valence-band calculation in Ref. 2 makes use of a semiempirical lateral mass $m^h_r/m_0=0.143$, whereas the noncoupling results (dashed line) in Fig. 2 are based on $m^h_r/m_0=1/(\gamma_1+\gamma_2)=0.094$. The use of a semiempirical mass in the single HH band calculation reduces the Zeeman effect and the calculated splitting of the luminescence line in Ref. 2 is somewhere in the middle of our coupled band and single HH band results.

The relative intensities of the corresponding luminescence lines are given in Fig. 3 as a function of field strength. Since the anticrossing of the levels $1\Pi^{+}_{\downarrow}$ and $1\Delta^{-}_{\uparrow}$ takes place around $B=2$ T, we present the relative intensities of both $1\Pi^{+}_{\downarrow}\rightarrow 1\Pi^{+}_{\downarrow}$ and $1\Pi^{+}_{\downarrow}\rightarrow 1\Delta^{-}_{\uparrow}$ luminescence lines. The simple structure of the intensity distribution in the coupled band calculations is due to the approximate conservation of mesoscopic angular momentum and spin in the interband transitions. The luminescence spectrum is dominated by transitions that take place between states having the same principal quantum number, mesoscopic angular momentum, and spin.The transitions that do not satisfy the approximate conservation laws are very weak, i.e., (i) transitions between states having the same symmetry but different principal quantum number, such as $2\Sigma_{\uparrow}\rightarrow 1\Sigma_{\uparrow}$ and (ii) transitions between states with different symmetry, such as $1\Pi^{+}_{\uparrow}\rightarrow 1\Pi^{-}_{\uparrow}$. The former are weak because of the almost perfect orthogonality of the lowest electron and valence-band states having the same mesoscopic angular momentum. At $B=0$, the relative intensity of the indirect transition $I(2\Sigma_{\uparrow}\rightarrow 1\Sigma_{\uparrow})$ is 0.008, whereas for a typical direct transition, $I(1\Sigma_{\uparrow}\rightarrow 1\Sigma_{\uparrow})=0.432$. Transitions which would correspond to an approximate spin flip are strictly forbidden because of the vanishing of the dipole moments. In contrast, there is a finite probability for the change of the mesoscopic angular momentum in the luminescence emission, e.g., $I(1\Pi^{+}_{\downarrow}\rightarrow 1\Pi^{-}_{\downarrow})=0.003$. The relative intensities are small because the envelope functions in the overlap integral have approximately different parities in the z direction. Except for the anticrossing states, the changes in the line intensities are fairly small for $B<6$ T. Since the indirect transitions are not strictly forbidden, they may be visible in spectral regions where there are no direct transitions.

[1] H. Lipsanen, M. Sopanen, and J. Ahopelto, Phys. Rev. B **51**, 13 868 (1995).

[2] R. Rinaldi, P. V. Giugno, R. Cingolani, H. Lipsanen, M. Sopanen, J. Tulkki, and J. Ahopelto, Phys. Rev. Lett. **77**, 342 (1996).

[3] M. Bayer *et al.*, Phys. Rev. Lett. **74**, 3439 (1995).

[4] T. Darnhofer, U. Rössler, and D. A. Broido, Phys. Rev. B **52**, R14 376 (1996).

[5] D. A. Broido, A. Cross, and U. Rössler, Phys. Rev. B **45**, 11 395 (1992); T. Darnhofer, D. A. Broido, and U. Rössler, *ibid.* **50**, 15 412 (1994).

[6] J. Tulkki and A. Heinämäki, Phys. Rev. B **52**, 8239 (1995).

[7] J. M. Luttinger and W. Kohn, Phys. Rev. **97**, 869 (1955); J. M. Luttinger, *ibid.* **102**, 1030 (1956).

[8] G. E. Pikus and G. L. Bir, Fiz. Tverd. Tela (Leningrad) **1**, 154 (1959) [Sov. Phys. Solid State **1**, 136 (1959)].

[9] M. Bayer, V. B. Timofeev, T. Gutbrod, A. Forchel, R. Steffen, and J. Oshinowo, Phys. Rev. B **52**, R11 623 (1995).